ULTA-HIGH TEMPERATURE CERAMIC COMPOSITES FOR LEADING EDGES

Stanley R. Levine, Mrityunjay Singh*, Elizabeth J. Opila, Jonathan A. Lorincz+, Jeanne Petko*, Donald T. Ellerby^, and Matthew J. Gasch#

*QSS Group Inc., NASA Glenn Research Center, Brookpark, OH
NASA Glenn Research Center, Brookpark, OH
+Ohio University, Athens, OH
^NASA Ames Research Center, Moffet Field, CA
Eloret, NASA Ames Research Center, Moffet Field, CA

ABSTRACT

Ultra-high temperature ceramics (UHTC) have performed unreliably due to material flaws and attachment design. These deficiencies are brought to the fore by the low fracture toughness and thermal shock resistance of UHTC. If these deficiencies are overcome, we are still faced with poor oxidation resistance as a limitation on UHTC applicability to reusable launch vehicles. We have been addressing the deficiencies of UHTC for the past two years via a small task at GRC that is in the Airframe part of the Next Generation Launch Technology Program. Our focus is on composite constructions and functional grading to address the mechanical issues and on composition modification to address the oxidation issue. The progress on approaches to improving oxidation resistance by alloying and functional grading will be reported. In particular, initial tests of tantalum additions have shown potential for major improvement. Less promising results of additional tests at higher temperatures will be presented. Two fabrication approaches are being pursued to produce carbon fiber reinforced UHTC composites: prepregging and rigid perform infiltration. Fabrication procedures and microstructures for composites will be reported

INTRODUCTION

The high melting points of refractory metal diborides coupled with their ability to form refractory oxide scales give these materials the capability to withstand temperatures in the 1900 to 2500°C range.[1] These ultra-high temperature ceramics (UHTC) were developed in the 1960's[2]. Fenter[3] provides a comprehensive review of the work accomplished in the 1960's and early 1970's. Additions of silicon carbide are used to enhance oxidation resistance and limit diboride grain growth. Carbon is also sometimes used as an additive to enhance thermal stress resistance. These materials offer a good combination of properties that make them candidates for airframe leading edges on sharp-bodied reentry vehicles.[1] UHTC have some potential to perform well in the environment for such applications, i.e. air at low pressure. However, for hypersonic flight in the upper atmosphere one must recognize that stagnation pressures can be greater than one atmosphere. Thus their poor oxidation resistance can be an issue.[4] Unreliable behavior under severe thermal shock and gradient loads or at attachments that results from low fracture toughness and large scatter in material properties is also an issue.[4]

At very high temperatures in a flowing environment most of the B_2O_3[5] and SiO_2[6] will be lost by evaporation or active oxidation. Thus, the primary protective oxidation barrier for the refractory metal borides is the refractory metal oxide scale plus any residual B_2O_3 and SiO_2. In the case of ZrB_2 or HfB_2 we are dependent on ZrO_2 or HfO_2, respectively. Background information on these oxides can be found in the compilation edited by Alper[7]. These oxides, if perfect, would be good oxygen barriers. However, ZrO_2 and HfO_2 become nonstoichiometric by forming oxygen lattice vacancies under low oxygen partial pressure conditions. They are also readily modified by aliovalent cations of lower valence to form

---

Distribution Statement: Approved for public release; distribution is unlimited.

This work was supported by the Airframe Technology Project, part of NASA's Next Generation Launch Technology Program.

oxygen lattice vacancies. Oxygen lattice vacancies allow rapid oxygen ion transport through the scale. So, from a chemistry perspective, ZrO_2 and HfO_2 are not good choices for a protective oxide scale. Another issue with ZrO_2 and HfO_2 scales is their phase instability. At high temperatures, ZrO_2 and HfO_2 are tetragonal. Upon cooling to room temperature they transform to the monoclinic structure with an attendant volume expansion. This phase transformation coupled with their high thermal expansion coefficient, and low thermal conductivity[8] can easily lead to cracking and spalling under thermal transient conditions.

One approach to resolve the oxygen transport issue and the cracking and spalling issue is to modify the scale with a cation that can stuff oxygen into the lattice and increase scale adhesion by phase stabilization. Thus we seek cations with higher valence. In addition, these cations must form a refractory oxide and they must also be derived from a refractory phase. The best candidates are niobium and tantalum. However, niobium pentoxide melts at only 1460°C[8]. That leaves tantalum, with a pentoxide melting point of 1880°C[7], as the only viable candidate to add to the refractory metal diborides. Additions can be either as the element, carbide, silicide or boride. Evidence that Ta additions to zirconia decrease conductivity is given by Kotlyar et al[9]. The choice of tantalum as an additive to the diborides is not new. Wuchina et al looked at TaB additions to HfC, HfN, and HfB_2.[10] They reported an increase in oxide scale density at 1500°C for HfB_2. Talmy et al studied up to 20 % additions of TaB_2 to ZrB_2 - 20 % SiC.[11] Furnace oxidation temperatures up to only 1400°C were used. They reported significant improvements in oxidation resistance and attributed these improvements to phase separation in the glass. In addition to Ta acting as a ZrO_2 or HfO_2 scale dopant or Ta_2O_5 acting as a glass modifier, one additional factor needs to be considered for Ta additions to the diborides. If Ta_2O_5 were a major oxide scale constituent it could form an intermediate phase with ZrO_2 (or possibly with HfO_2) with a nominal composition of $Ta_2O_5 \cdot 6ZrO_2$. This intermediate phase has a lower melting point than either pure oxide.[12] Its presence could be either beneficial or detrimental. The approach chosen for oxidation resistance enhancement is the addition of tantalum via refractory compounds (melting points in parentheses): Ta_5Si_3 (2460°C) [13], $TaSi_2$ (2200°C) [14], TaC (3880°C) [14], TaB (2040°C) [14] or TaB_2 (3140°C) [14]. This paper deals only with $TaSi_2$ additions.

One means of for possibly overcoming these issues is to introduce fibers as a toughening and strengthening phase, and as a pathway to architectural tailoring of properties such as thermal conductivity, stiffness, strength, etc. Fiber choices at this time are limited to carbon. This introduces new problems such as the need for new processing approaches, oxidation of the reinforcing phase, and thermal expansion mismatch between the carbon fibers and the UHTC matrix to name just a few.

The purpose of this study was to examine approaches to resolving the oxidation and reliability issues. Alloying approaches are being examined to improve oxidation resistance. Fiber reinforcement and functional grading are being examined to increase toughness and improve reliability. These approaches are being integrated to develop UHTC materials with improved robustness for leading edge applications. The status of these approaches for improving UHTC robustness is reported in this paper.

EXPERIMENTAL PROCEDURES

Specimens of baseline ZrB_2 - 20 v/o SiC and ZrB_2 - 20 v/o SiC - 20 v/o $TaSi_2$ were prepared following conventional powder preparation and hot pressing procedures[15] to reach > 95% of theoretical density. After pressing, the plates were removed from the die, scraped to remove residual grafoil, and then machined into oxidation coupons and flexural test specimens per ASTM Standard.[16] Oxidation coupons were 2.54 by 1.27 by 0.32 cm. Weighed and measured samples were loaded into a slotted ZrO_2 refractory brick. Samples were exposed to ten-minute oxidation cycles in stagnant air at 1627 or 1927°C. One sample was removed after one cycle, five cycles and ten cycles. A maximum exposure time of 100 minutes was thus achieved. Weight change was measured, where possible. Some of the samples stuck to the sample holder during oxidation due to extensive glass formation. X-ray diffraction (XRD) was used to identify oxide phases present after exposure. After surface microstructural analysis by scanning electron microscopy (SEM) and X-ray energy dispersive spectroscopy (XEDS), samples were cross-sectioned and polished in non-aqueous 1μm diamond polishing media. Water was avoided to preserve any boria that might be present as an oxidation product.

A button shaped arc jet specimen was also prepared by hot pressing, and finish machining. The sample was exposed in an arc jet at NASA Ames Research Center. Conditions were 350 W/m^2, 0.07 atm, 600 seconds.

RESULTS AND DISCUSSION

OXIDATION RESISTANCE WITH TANTALUM ADDITIONS

Figure 1 shows the macroscopic appearance of specimens for ZrB_2 – 20 v/o SiC and ZrB_2 - 20 v/o SiC – 20 v/o $TaSi_2$ exposed at 1627°C for 1, 5 and 10 ten-minute cycles. The ZrB_2 - 20 v/o SiC

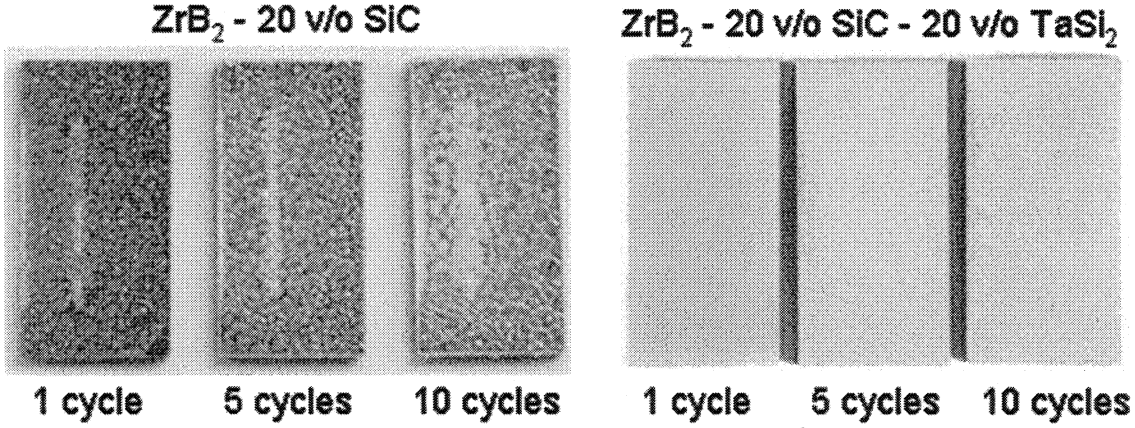

Figure 1. UHTC oxidized in air at 1627°C

specimens were generally uniform in appearance except for the areas in contact with the zirconia setter along one edge and along a line to the left of center down the face. Here less oxidation occurred. The ZrB_2 - 20 v/o SiC - 20 v/o $TaSi_2$ performed very well, forming a uniform compact oxide scale. These macroscopic observations are supported by the oxidation results shown in Figure 2. The oxidation kinetics are close to parabolic. Oxidation was significantly slower for ZrB_2 - 20 v/o SiC - 20 v/o $TaSi_2$.

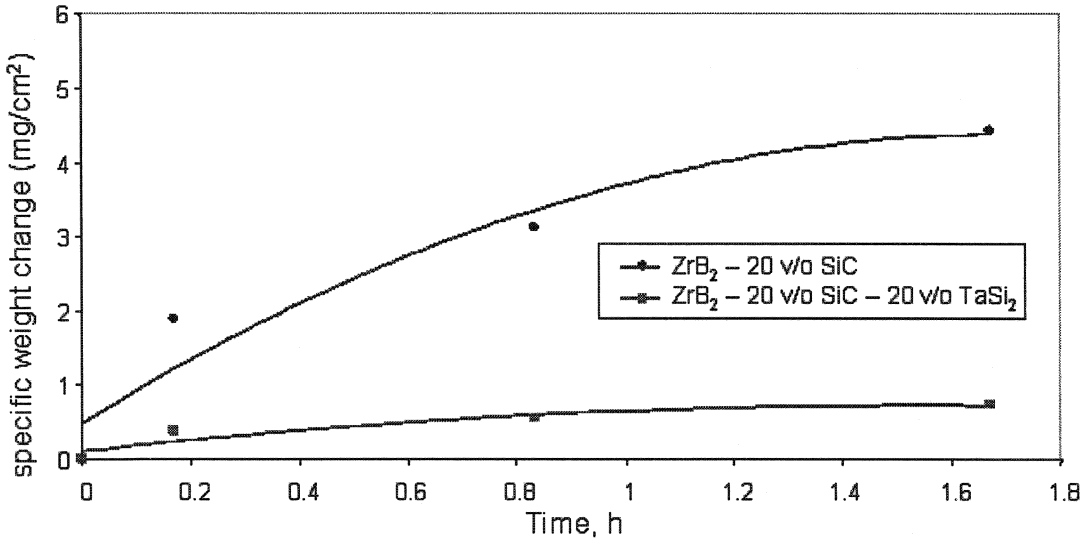

Figure 2. UHTC oxidation at 1627°C

Figure 3 shows the appearance of ZrB_2 - 20 v/o SiC after exposures for 1, 5, and 10 ten minute cycles at 1927°C. Samples oxidized at 1927°C formed an orange oxide after one 10-minute cycle. With increasing exposure time, the oxide scale became grayer. At this exposure temperature, swelling of the samples occurred with the thickness of the specimens increasing by up to 80% after ten 10-minute

cycles. Extensive distress in the form of cracks, nodules, and spallation is evident. From a cross-section it was determined that the sample exposed at 1927°C for ten 10-minute cycles is almost completely consumed. Here, the oxide scale was several mm thick. The scale was composed of large ZrO_2 grains in a silica-rich glassy phase. No SiC depletion layer was observed.

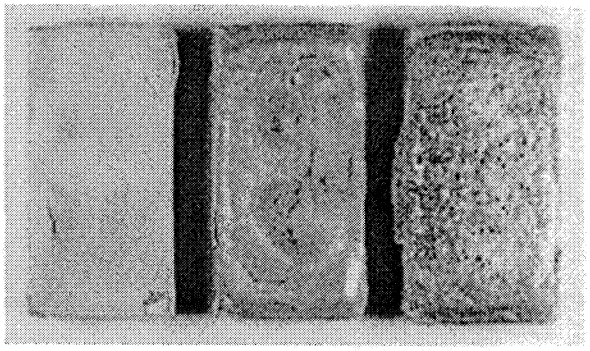

Figure 3. ZrB_2 - 20 v/o SiC after exposures for 1, 5, and 10 ten-minute cycles at 1927°C.

Figure 4 shows the macroscopic appearance of ZrB_2 - 20 v/o SiC - 20 v/o$TaSi_2$ after 1 and 5 ten-minute cycles of exposure at 1927°C. Sample distress is evident at the edges after one cycle. A

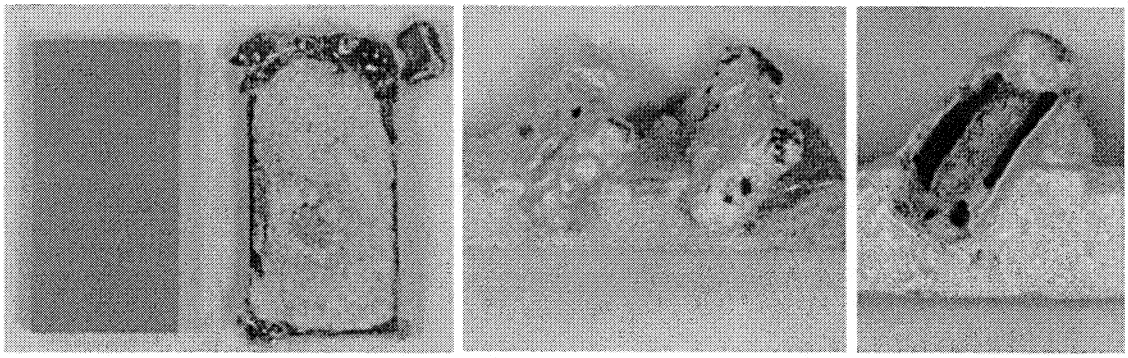

(a) as-received and ten minutes **(b) 5 ten m cycles in setter** **(c) 5 ten m cycles**

Figure 4. ZrB_2 - 20 v/o SiC - 20 v/o$TaSi_2$ after 1 and 5 ten-minute cycles of exposure at 1927°C

large amount of low viscosity glass was generated after 5 cycles. The glass firmly bonded the samples to the zirconia setter, so weight change versus time data were not obtained. In Figure 4(c) a photo of the specimen edge is shown where the sample was broken during attempted removal from the setter. The large gap between the sample and scale is evidence of significant material consumption. Metallographic characterization is planned.

Figure 5 shows the cross-sectional microstructure of ZrB_2 - 20 v/o SiC - 20 v/o$TaSi_2$ after 1 and 10 ten-minute cycles of exposure at 1627°C. A dense, compact and adherent scale is present in both instances. X- ray diffraction results show formation of monoclinic ZrO_2 as the major phase with minor amounts of cubic ZrO_2 present. X-ray energy dispersive spectroscopy (EDS) shows SiO_2 present

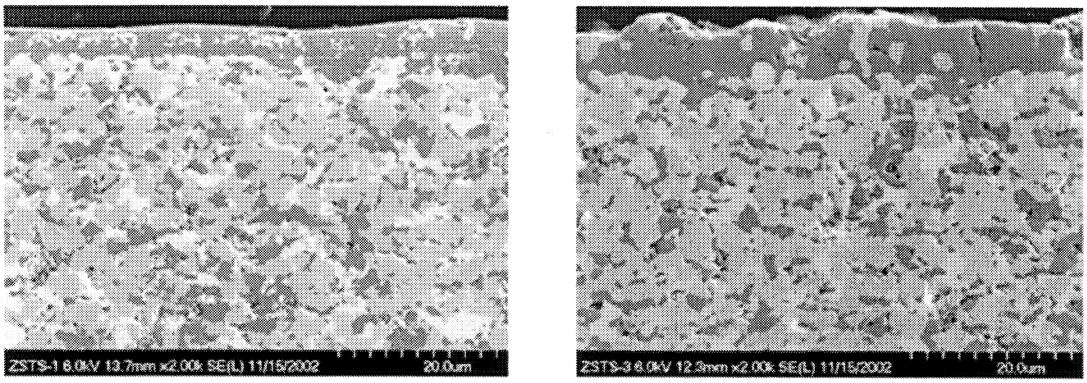

1x10 min cycle **10x10min cycles**

Fig. 5. ZrB_2 - 20 v/o SiC - 20 v/o$TaSi_2$ after 1 and 10 ten-min. 1627°C cycles

with ZrO_2 particles. No oxides of Ta were detected, but Ta may be dissolved in ZrO_2 or SiO_2 with other impurities. Also, Ta is difficult to detect due to peak overlaps with Si. Wave length dispersive spectroscopy is planned to overcome this difficulty.

Figure 6 compares the microstructures of the oxide scales formed on ZrB_2 - 20 v/o SiC - 20 v/o $TaSi_2$ with that formed on a commercially prepared ZrB_2 - 20 v/o SiC after 10 ten-minute cycles of exposure at 1627°C. The difference is striking. On the latter the outer oxide layer, mostly SiO_2, is about 10 times thicker than on the ZrB_2 - 20 v/o SiC - 20 v/o $TaSi_2$. The total thickness of the scale and the two

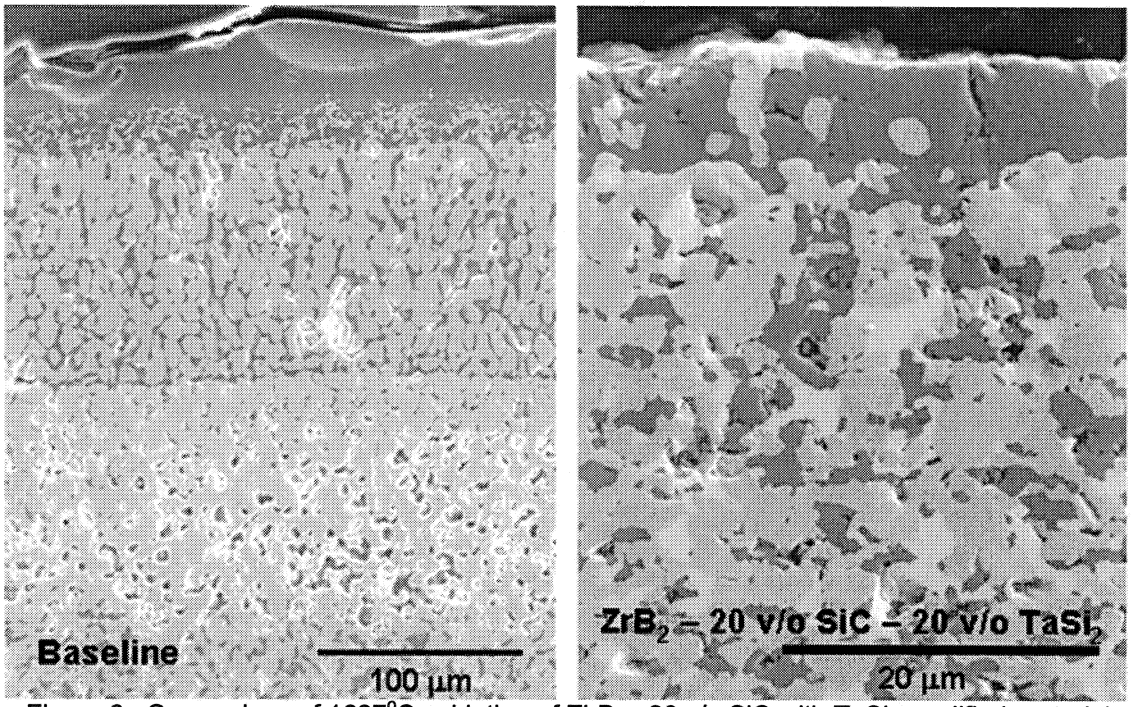

Figure 6. Comparison of 1627°C oxidation of ZbB_2 - 20 v/o SiC with $TaSi_2$ modified material

depleted zones is 258 ± 85 µm for the ZrB_2 - 20 v/o SiC on the side shown based on the average of 13 measurements. On the other side the scale plus depleted zone was 515 ± 253 µm based on the average of 12 measurements. The average for the 25 total measurements was 381 ± 224 µm. In the ZrB_2 - 20 v/o SiC - 20 v/o $TaSi_2$ the total thickness of the scale was 6.3 ± 1.6µm. A depleted zone was not apparent.

The appearance of the arc jet specimen, the specimen mounted in the specimen holder, and the assembly mounted in the sting are shown in Figure 7. Temperature measurements in the arc jet test indicated that 1800 to 1960°C was attained. Based on observations from many tests it can also be stated that the edge of the specimen runs hotter than the center since more oxidation has been observed at specimen edges. Heat flux models indicate as much as a 70% higher heat flux near the specimen edge. Therefore, the edge temperature could be considerably higher than the 1800 to 1960°C center temperature. The tested sample is shown in Figure 8. The oxide scale appears to be adherent, but with obvious melting and flow near the edges. Higher magnification views of the center and edge region are shown in Figure 9. There are pinhole pores typical of ZrB_2 + SiC oxidized at high temperature. The incidence of pores is greater at the hotter specimen edge. Evidence of melting and flow of the oxide scale is also apparent. X-ray diffraction (XRD) analysis of the central part of the specimen detected monoclinic ZrO_2 and possibly highly oriented cubic ZrO_2 as major phases. Also, Ta_2O_5 was a possible third major phase. XRD results for some material ground from a piece that broke from the edge during handling detected only monoclinic ZrO_2 and possibly highly oriented cubic ZrO_2 as major phases.

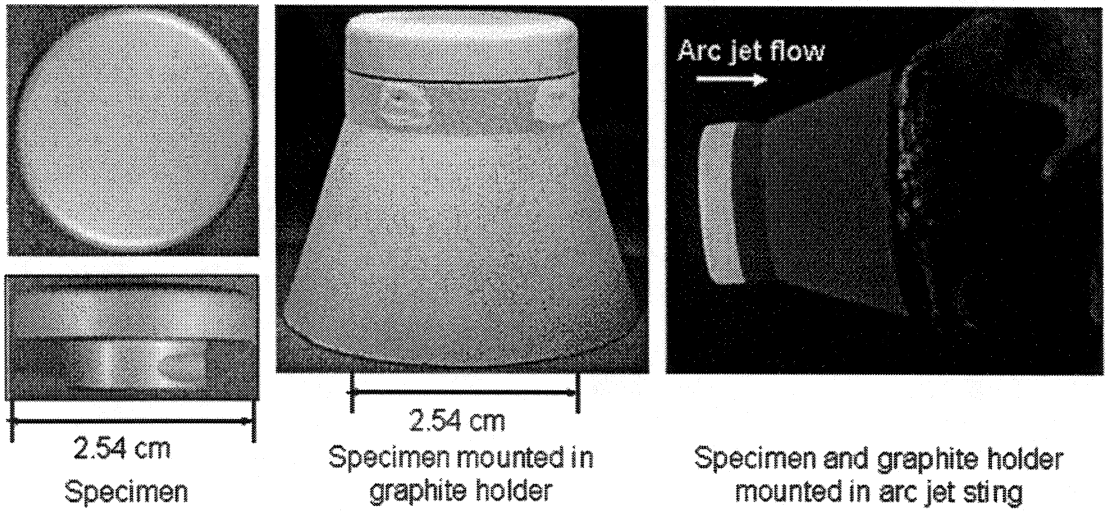

Figure 7. Arc jet test specimen and specimen mounting fixtures

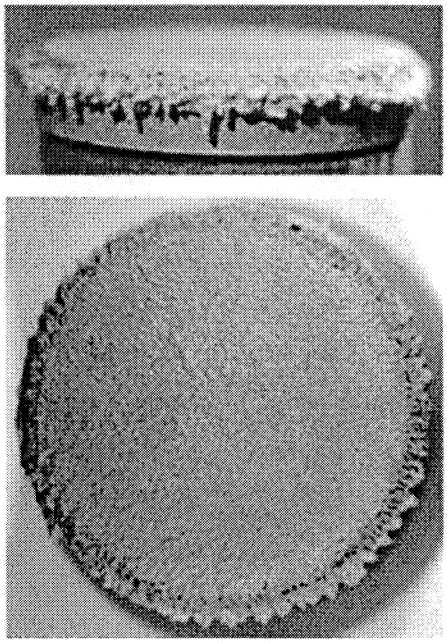

Figure 8. (Above) ZrB_2 - 20 v/o SiC - 20 v/o $TaSi_2$ after arc jet test

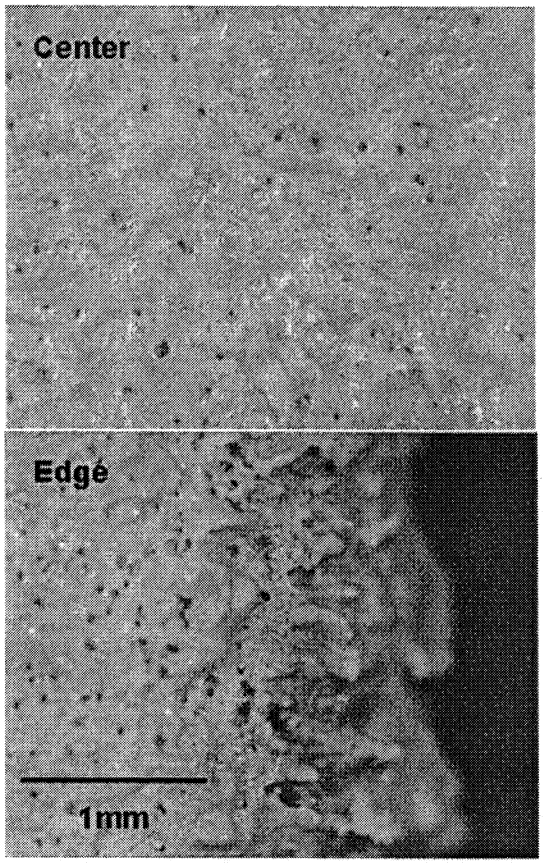

Figure 9. (At right) Higher magnification photographs of ZrB_2 - 20v/o SiC - 20 v/o $TaSi_2$ after arc jet test

Field emission scanning electron microscopy was performed on the arc jet sample. The photos on the left of Figure 10 show areas near the center of the specimen. EDS of area C indicates the strong presence of ZrO_2 with Si, Ta, and B also present as oxide. EDS of area D detected SiO_2 with Zr and Si as oxide also present. The photo at the upper right is a section through the outer oxide scale where a piece spalled during handling. The location is estimated to be about 0.5 cm from the specimen edge. Large pores throughout the scale are seen, but it cannot be determined if they provide a continuous path through the scale. An area exposed by the spall is shown at the lower right of Figure 10. EDS of area A detected Ta_2O_5 with some Si oxide present. EDS of area B indicated the presence of ZrO_2 with

significant Ta also present as oxide. Non-aqueous metallographic preparation of the specimen in cross-section is underway.

UHTC COMPOSITES

Monolithic UHTC materials such as HfB_2 + SiC and ZrB_2 + SiC have low fracture toughness and relatively poor thermal shock resistance compared to structural ceramics such as the advanced sintered silicon nitrides. Thus one can expect difficulties with issues such as response to thermal stress and thermal shock, and structural integrity at critical areas such as attachments to the airframe or inlet structure[4]. We have begun to explore UHTC Composites (UHTCC) by two approaches: 1) evaluation of

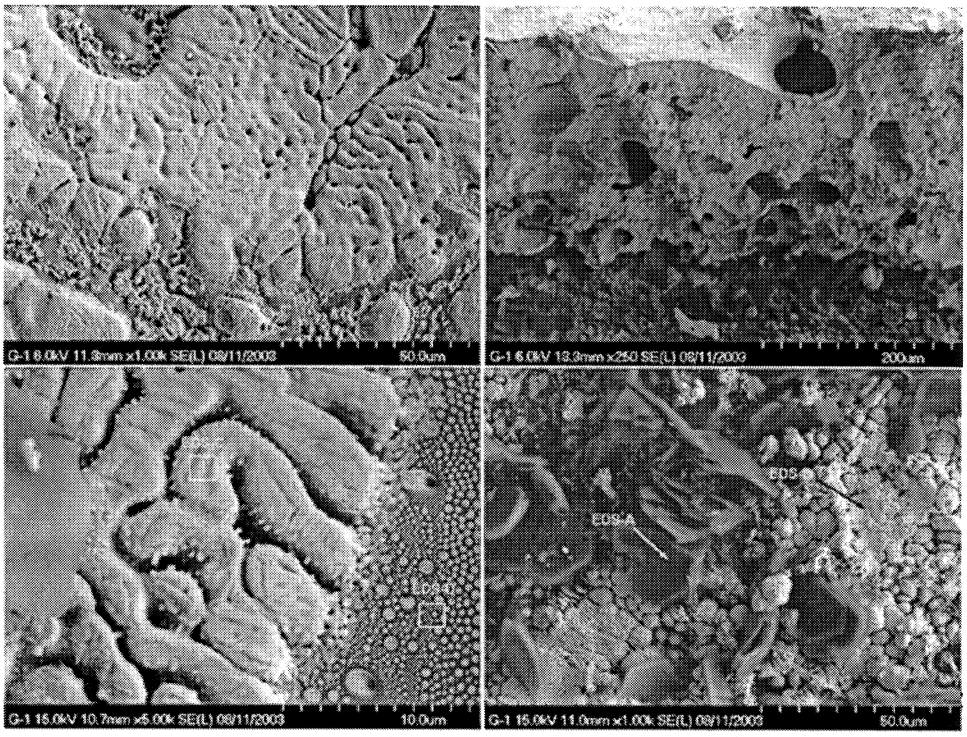

Figure 10. FESEM images of the surface of Zr B_2 - 20 v/o SiC - 20 v/o $TaSi_2$ after arc jet test. Upper and lower left photos are of an area near the center of the specimen; upper right is a scale cross section at the edge of the spall; lower right is an area exposed near the edge in the spalled area.

vendor produced materials, and 2) processing in house via melt infiltration technology as potential solutions.

The first commercially produced material that we are examining was assembled by Starfire Systems Inc. for NASA Langley. The processing involved slurry impregnation followed by polymer infiltration and pyrolysis. The microstructure of this material along with XRD results are shown in Figure 11. The material was received in the form of a 15 x 15 x 0.6 cm hot pressed plate. From this plate we were able to extract a limited number of flexural strength test bars, some coupons for furnace oxidation, and two 5 x 5 cm plates for a torch test. Results of testing are reported elsewhere.[17]

At GRC, two innovative composite processing approaches are being developed. These approaches are based on either the prepreg and melt infiltration (PREMI) technology, or a ceramic hybrid approach to form functionally graded UHTC layers on carbon fiber reinforced ultra-high temperature ceramic matrix composites. In both of these techniques, a reactive melt infiltration based approach is used. Both fabrication approaches are flexible enough to allow oxidation resistant phases to be incorporated at different processing steps. In this paper, processing details and microstructure of ultra-

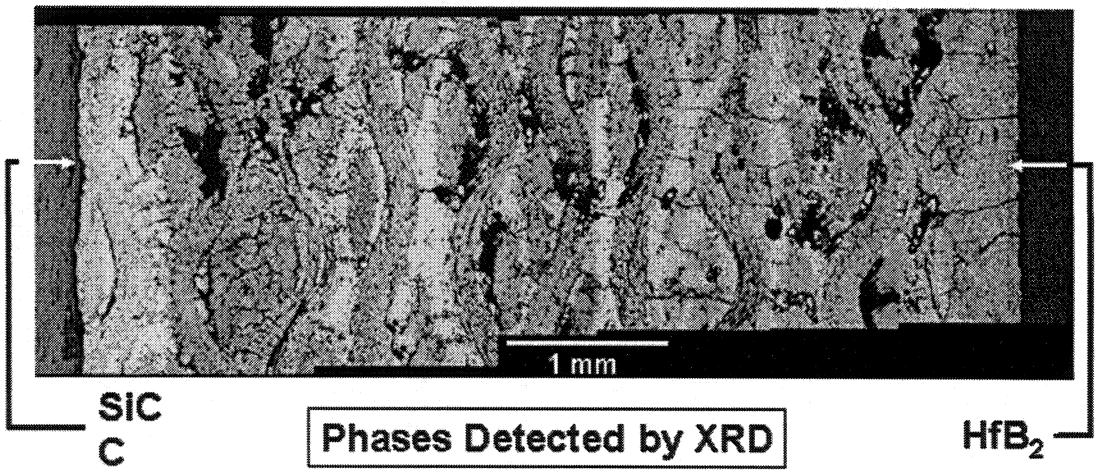

Figure 11. Starfire UHTCC as-produced microstructure

high temperature ceramic composites fabricated by the prepreg and melt infiltration approach will be discussed.

The fabrication approach involves three steps. In the first step, woven T-300 (5-HS, 3K tow) carbon fiber cloth is prepregged in a polymer mixture, which is a combination of a monomer, pore former, carbon source, refractory compounds, dispersant, and a catalyst. This carbon fiber cloth is usually pre-coated with an interface coating to protect the fibers from oxidation. In this case a BN interface coating was applied(Synterials Inc., VA MOD-1 coating). The carbon cloth is prepregged with the polymer mixture and cured in an oven at 60°C for approximately one hour. The time in the oven depends on when the prepreg mixture attains the right amount of tackiness. Before removal from the oven, the tackiness is checked to determine that it is not too wet. At this point the composite can be molded into a specific form and thickness. In the second step of this process, 8 or 10 layers of prepregged cloth are cut out, layed-up within a steel mold and vacuum bagged. Warm pressing is then carried out at 110°C followed by pyrolysis at up to 1000°C in flowing argon. In the pyrolysis process, the polymer converts to carbon and the pore former leaves an interconnected network of porosity. This porosity is very critical for the complete infiltration and reaction of carbon with refractory metal-silicon alloys. The final step of the fabrication process involves the reactive melt infiltration of refractory metal-silicon alloys leading to ultra-high temperature matrix materials.

Figure 12 (a) shows the microstructure of a Ta-Si melt infiltrated composite. Figure 12 (b) and (c) show carbon fiber reinforced UHTC composites with ZrB_2 and SiC particulates in the matrix. There is cracking observed in the final composite materials due to thermal expansion mismatch between carbon fibers

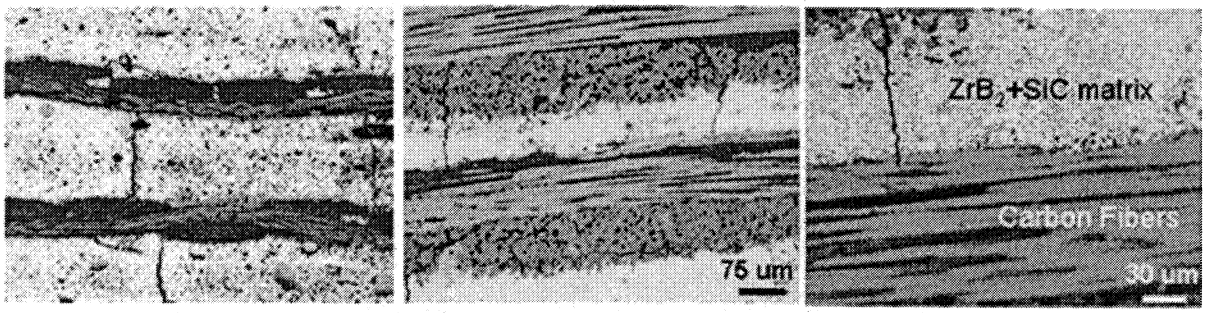

Figure 12. Microstructure of carbon fiber reinforced UHTC composites. (a) Ta-Si infiltrated composite. (b) and (c) are UHTC composites with ZrB_2 and SiC phases in the matrix.

and ultra-high temperature composite matrix constituents. Experimental efforts will be needed to assess the conditions under which these cracks close. Sealants may also have to be investigated.

SUMMARY AND CONCLUSIONS

In this study approaches for improving the oxidation resistance and thermomechanical durability of UHTC have been investigated. We have found that $TaSi_2$ additions are beneficial at 1627°C. At higher temperatures, in an arc jet test and at 1927°C in a furnace test, we have seen dramatic evidence that 20 v/o $TaSi_2$ addition to ZrB_2 - 20 v/o SiC is extremely detrimental due to the formation of a low melting phase. In the area of composites, the fabrication approaches that we have examined in commercial materials and in-house produced materials have resulted in matrix cracked materials as one might expect from the thermal expansion mismatch between carbon fibers and the various matrix constituents. The significance of this at use temperatures that will be at or above the fabrication temperature is yet to be determined. At lower temperatures, sealants will be needed.

FUTURE WORK

Future work in the area of oxidation will focus on lower levels of Ta addition to achieve scale doping without introducing significant free tantala to form low melting phases. Composites work will continue to examine commercially produced UHTCC and place emphasis on characterization for mechanical properties and oxidation resistance.

ACKNOWLEDGMENTS

The authors are grateful for the assistance of Raymond Babuder and Robert C. Angus for assistance with processing, Ronald E. Phillips and Raymond C. Robinson for assistance with testing, and Terry R. McCue for FESEM analysis. We also gratefully acknowledge the contributions of Sarah E. Beckman, and Jerome W. Ridge (ELORET) of NASA Ames Research Center for the arc jet testing.

REFERENCES

1. Bull, J.D., Rasky, D.J. & Karika, C.C., ***Stability characterization of diboride composites under high velocity atmospheric flight conditions***. 24th International SAMPE Technical Conference, 1992, pp. T1092- T1106.

2. Clougherty, E.V., Pober, R.L. & Kaufman, L., ***Synthesis of oxidation resistant metal diboride composites.*** Trans. Met. Soc. AIME, 1968, 242, 1077-1082.

3. Fenter, J.R., ***Refractory diborides as engineering materials.*** SAMPE Quarterly, 1971, 2, 1-15.

4. Levine, S.R., Opila, E.J., Halbig, M.C., Kiser, J.D., Singh, M., and Salem, J.A., ***Evaluation of ultra-high temperature ceramics for aeropropulsion use.*** J. European Ceramic Soc., 2002, 22, pp. 2757-2767.

5. Tripp, W.C., Davis, H.H. & Graham, H.C., ***Effect of an SiC addition on the oxidation of ZrB_2.*** *Cer.* Bull., 1973, 52, 612-616.

6. Opila, E.J. & Halbig, M.C., ***Oxidation of ZrB_2-based ultra-high temperature ceramics.*** Ceramic Engineering and Science Proceedings, 2001, 22 # 3, 221-8.

7. Alper, A.M., ***High Temperature Oxides, Part II: Oxides Of Rare Earths, Titanium, Zirconium, Hafnium, And Tantalum.*** Academic Press, New York,1970. Garvie, R.C., ***Zirconium dioxide and some of its binary systems, Chapter IV.*** Lynch, C.T., *Hafnium oxide*, Chapter VI.

8. Anon., ***Engineering property data on selected ceramics, Vol. III, Single oxides***. MCIC-HB-07, Battelle, Columbus, OH, 1981.

9. Kotlyar, A.G., Neuimin, A.D., Pal'guev, S.F., Strekalovskii, V.N., and Zubankov, V.N., ***Structure and electrical conductivity in the system ZrO2-Y2O3-Ta2O5***. translated from Izvestia Akademii Nauk SSR, Neorganicheskie Materialy, 1970, 6, 327-331.

10. Wuchina, E.J. and Opeka, M.M., ***The oxidation of HfC, HfN and HfB_2.*** Electrochemical Soc. Proceedings, 2001#12, 136-43.

11. Talmy, I.G., Zaykoski, J.A., Opeka, M.M., and Dallek, S., ***Oxidation of ZrB_2 ceramics with SiC and Group IV – VI transition metal diborides.*** Electrochemical Soc. Proceedings, 2001#12, 144-58.

12. Levin, E.M., Robbins, C.R., and McMurdie, H.F., ***Phase Diagrams for Ceramists,*** The American Ceramic Soc., Inc., Columbus, OH, 1964, p. 144.

13. Shaffer, P.T., ***Handbooks of High Temperature Materials, #1, Materials Index.*** Plenum Press, New York, 1964, p. 580.

14. ***Handbook of Chemistry and Physics***. D. R. Lide, Editor, CRC Press, New York, 1997, Section 4, p. 89.

15. ASTM C 1161-02, **Standard Test Method For Flexural Strength Of Advanced Ceramics At Ambient Temperature**. *Annual Book of ASTM Standards, V. 15.01-02,* American Society for Testing and Materials, West Conshohocken, Pennsylvania (2002).

16. Levine, S.R. and Opila, E.J., ***Tantalum addition to zirconium diboride for improved oxidation resistance***. NASA/TM- 2003-212483, July, 2003.

17. Levine, S.R., Opila, E.J., Robinson, R.C., and Lorincz, J.A., ***Characterization of an ultra-high temperature ceramic composite***. 55th Pacific Coast Regional & Basic Science Division Fall Meeting, October 19 - 22, 2003, Oakland, CA.